HHS Public Access

Author manuscript

J Bone Miner Res. Author manuscript; available in PMC 2021 August 01.

Published in final edited form as:

J Bone Miner Res. 2020 August ; 35(8): 1494–1503. doi:10.1002/jbmr.4018.

Connexin 43 Is Necessary for Murine Tendon Enthesis Formation and Response to Loading

Hua Shen[1], **Andrea G Schwartz**[1], **Roberto Civitelli**[2], **Stavros Thomopoulos**[3,4]

[1]Department of Orthopaedic Surgery, Washington University, St. Louis, MO, USA

[2]Department of Internal Medicine, Division of Bone and Mineral Disease, Washington University, St. Louis, MO, USA

[3]Department of Orthopedic Surgery, Columbia University, New York, NY, USA

[4]Department of Biomedical Engineering, Columbia University, New York, NY, USA

Abstract

The enthesis is a mineralized fibrocartilage transition that attaches tendon to bone and is vital for musculoskeletal function. Despite recent studies demonstrating the necessity of muscle loading for enthesis formation, the mechanisms that regulate enthesis formation and mechanoresponsiveness remain unclear. Therefore, the current study investigated the role of the gap junction protein connexin 43 in these processes by deleting *Gja1* (the Cx43 gene) in the tendon and enthesis. Compared with their wild-type (WT) counterparts, mice lacking Cx43 showed disrupted entheseal cell alignment, reduced mineralized fibrocartilage, and impaired biomechanical properties of the supraspinatus tendon entheses during postnatal development. Cx43-deficient mice also exhibited reduced ability to complete a treadmill running protocol but no apparent deficits in daily activity, metabolic indexes, shoulder muscle size, grip strength, and major trabecular bone properties of the adjacent humeral head. To examine enthesis mechanoresponsiveness, young adult mice were subjected to modest treadmill exercise. *Gja1* deficiency in the tendon and enthesis reduced entheseal anabolic responses to treadmill exercise: WT mice had increased expression of *Sox9*, *Ihh*, and *Gli1* and increased Brdu incorporation, whereas Cx43-deficient mice showed no changes or decreased levels with exercise. Collectively, the results demonstrated an essential role for Cx43 in postnatal tendon enthesis formation, function, and response to loading; results further provided evidence implicating a link between Cx43 function and the hedgehog signaling pathway.

Keywords

CONNEXIN 43; ENTHESIS; GAP JUNCTION; GLI1; TENDON

Address correspondence to: Stavros Thomopoulos, PhD, Department of Orthopedic Surgery, Department of Biomedical Engineering, 650 West 168th Street, Black Building 1408, New York, NY 10025, USA. sat2@columbia.edu.

Authors' roles: Study design: HS and ST. Study conduct: HS and AGS. Data analysis: HS and AGS. Data interpretation: HS, ST, AGS, and RC. Drafting manuscript: HS. Revising manuscript content: HS, RC, and ST. Approving final version of manuscript: HS, AGS, RC, and ST. HS and ST take responsibility for the integrity of the data analysis.

Disclosures

All authors state that they have no conflicts of interest.

Additional Supporting Information may be found in the online version of this article.

Introduction

The tendon enthesis is a complex fibrocartilaginous tissue bridging tendon and bone. It dissipates stress concentrations and enables effective load transfer between muscle and bone, and is thus vital for musculoskeletal function.[1,2] The tissue is prone to overload-induced injuries but also relies on mechanical stimuli for its formation and maintenance.[3–5] We and others recently found that hedgehog/Gli1 signaling is necessary for establishing enthesis structure and biomechanics;[6–8] however, it remains unclear how mechanical stimuli are translated into intracellular signals that shape entheseal structure and strength.

Gap junction proteins are thought to be involved in transducing mechanical signals in musculoskeletal tissues.[9] Connexin 43 (Cx43), in particular, is one of the most abundant gap junction proteins expressed in skeletal tissues.[10,11] The basic functional unit of Cx43 is a hexamer, also known as a connexon or hemichannel. Two connexons from two apposing cells dock with each other to form a gap junction, thus enabling the propagation of nutrients and/or biochemical signals between connected cells and eliciting uniform cellular responses.[10,11] Undocked Cx43 hemichannels formed in unapposed cell membranes facing the extracellular environment may also mediate autocrine or paracrine regulation of target cell functions by releasing small molecules such as ATP and prostaglandin E2.[12,13] Additionally, Cx43 possesses a long intracellular C-terminus that can bind multiple signaling molecules, including PKC, ERK1, ERK2, and ß-catenin.[14,15] Therefore, Cx43 can modulate tissue structural and functional properties in response to dynamic changes in their local environment, including mechanical load, by tuning cell responsiveness to extracellular stimuli. Consistent with this, in vivo studies from a number of groups have demonstrated that Cx43 is essential in shaping bone microarchitecture and in regulating bone sensitivity to mechanical loading.[9,16–18]

In addition to bone cells, Cx43 is also expressed by tenocytes and enthesis cells.[19,20] An in vitro study showed that gap junction intercellular communication is necessary for tenocyte anabolic response to mechanical loading.[21] On the other hand, overexpression of Cx43 inhibited catabolic and pro-inflammatory responses in tenocytes against heat stress.[22] However, the in vivo roles and mechanisms of Cx43 in the tendon and tendon enthesis are largely unexplored. Therefore, this study aimed to investigate the role of Cx43 in postnatal tendon and enthesis formation and their response to loading using a mouse genetic model. We hypothesized that Cx43, similar to bone cells, is involved in the formation of a functional tendon enthesis and is necessary for the regulation of enthesis mechanoresponsiveness.

Materials and Methods

Mouse model and study design

The study was conducted in accordance with the Public Health Service Policy on Humane Care and Use of Laboratory Animals and approved by the Institutional Animal Care and Use Committee at Washington University in St. Louis. All mice were housed in groups in a 12-hour light/dark cycle with free access to standard rodent chow and fresh water. Conditional deletion of the Cx43 gene, *Gja1*, in the tendon and tendon enthesis was achieved by crossing $Gja1^{flox/flox}$ mice with $ScxCre;Gja1^{+/-}$ mice. The resulting conditional knockout mice (cKO,

ScxCre;*Gja1*$^{flox/-}$) and their wild-type equivalent (WT, *Gja1*$^{flox/+}$) were used in this study. The selectivity and efficiency of *Gja1* deletion were confirmed by crossing *ScxCre*;*ScxGFP* mice (provided by Dr Ronen Schweitzer) with the Ai14 Cre reporter mice (Jackson Laboratory, Bar Harbor, ME, USA)[23] and by immunostaining for Cx43 and real-time PCR for *Gja1* expression (Fig. 1). The age- and sex-matched WT and cKO mice of both sexes were randomly allocated to groups and compared for postnatal tendon and enthesis formation at the supraspinatus (SS) and Achilles tendons, biomechanical properties at the SS tendon-humerus unit, related musculoskeletal structure and function at the shoulder, mechanoresponsiveness at the Achilles tendon and enthesis after treadmill exercise, and overall mouse activity and metabolism. Specifically, tendon enthesis formation was assessed in 4-week- and 8- or 10-week-old mice by micro-computed tomography (μCT, n = 7~10/strain/age group) and histology (n = 4/strain/age group). Tendon enthesis biomechanical properties were determined in the 10-week-old mice (n = 7 and 9 for WT and cKO mice, respectively). Shoulder and rotator cuff structure and strength were evaluated in 4-week- and 8- or 10-week-old mice by μCT for SS muscle size and humeral bone microarchitecture (n = 7~10/strain/age group) and by grip test for upper limb strength (n = 9~11/strain/age group).[17] Achilles tendon enthesis mechanoresponsiveness was assessed in adult mice (14~15 weeks old) by gene expression analysis (n = 7~10/strain/condition) and histomorphormetry (n = 3~5/strain/condition). Overall mouse cage activity and metabolism were determined in 10-week-old WT (n = 3) and cKO mice (n = 4) in metabolic cages (PhenoMaster, TSE Systems, Bad Homburg, Germany) for 72 hours according to manufacturer's instructions.

Tendon, muscle, and bone morphometry (μCT)

A μCT40 scanner (Scanco Medical AG, Bruttisellen, Switzerland) was used to determine the maximum cross-sectional area (CSA) of SS muscles, the minimum CSA of SS tendons, the total volume of mineralized fibrocartilage of SS tendon entheses, and the trabecular bone properties (ie, total volume [TV], bone volume [BV], BV/TV, tissue mineral density [TMD], trabecular bone number [Tb.N], trabecular thickness [Tb.Th], and trabecular space [Tb. Sp]) at the metaphysis of humeral heads proximal to the growth plate.[17] Scans were conducted at 6 μm resolution, 45 kVp, 177 μA, and 250 ms integration time for the 4-week-old SS entheses, humeral heads, and SS tendons, at 12 μm resolution, 45 kVp, 177 μA, and 250 ms integration time for the 8-week-old humeral heads and SS entheses, and at 20 μm resolution, 45 kVp, 176 μA, and 300 ms integration time for all other samples. The mineralized fibrocartilage volume was determined by 3D evaluation of semi-automatically contoured slices that covers the full range of SS tendon enthesis with the lower threshold of segmentation set to 200 and 320 for 4-week and 8-week samples, respectively.

Tendon enthesis biomechanics

The biomechanical properties of WT and cKO mouse tendon entheses were determined at SS tendon enthesis via uniaxial tensile testing, as detailed elsewhere.[5] In brief, SS tendon attached to humerus was mounted between two custom grips that secure SS tendon and humerus, respectively, and tested in a 37°C phosphate-buffered saline (PBS) bath on an Instron ElectroPlus E1000 (Instron Corp., Canton, MA, USA) equipped with a 30 N load cell. The tendon gauge length was determined optically and the tendon minimum CSA was determined via μCT before the test. The testing protocol consisted of a 100 mN preload, 5

cycles of preconditioning using a triangle waveform with a peak load of 50 mN, and 5 minutes of relaxation followed by loading to failure at 0.5%/s. Tested tendons were imaged continuously throughout the testing protocol. Estimates of the stiffness/modulus were made from the load-displacement and stress-strain curves of each uniaxial tensile failure test. The stiffness/elastic modulus of each sample was determined from the linear portion of each load-displacement/stress-strain curve. The maximum force and stress were defined as the peak values on the force-displacement and stress-strain curves, respectively.

Response to treadmill exercise

Treadmill exercise was carried out on a level platform to assess the impact of Cx43 deficiency in the tendon and enthesis on tendon enthesis function and mechanoresponsiveness. All treadmill mice were pretrained at a speed of 6~10 m/min for 12 minutes per day for 3 consecutive days. After a 2-day rest, the trained mice were subjected to either of the following running protocols: (i) Intermediate-level treadmill running: 10-week-old cKO mice and their WT littermates were subjected to a single session of treadmill running at 10 m/min for 10 minutes followed by 12 m/min for additional 30 minutes to examine mouse running ability. Mice fell off of the running track when they were unable to keep up with the speed of the treadmill. The number of falls per mouse during the running session was counted and used as a metric of mouse running ability. (ii) Modest-level treadmill exercise: adult cKO mice and their WT littermates (14 to 15 weeks old) were subjected to a treadmill exercise consisting of 10 m/min for 30 minutes followed by 12 m/min for 10 minutes per day for 2 days to assess the mechanoresponsiveness of the tendon enthesis to treadmill running. Adult mice were used in this experiment because young cKO mice had difficulty completing the running protocol. To detect proliferating cells in vivo, some mice were given 0.8 mg/mL 5-bromo-2′-deoxyuridine (BrdU, Sigma-Aldrich, St. Louis, MO, USA) in drinking water immediately after the first running session until they were euthanized 24 hours after the last running session. All other mice were euthanized within 30 minutes after the last running session. Age- and sex-matched WT and cKO mice without treadmill running were handled and housed under the same conditions as those treadmill mice and used as cage controls.

RNA isolation and real-time PCR

Total RNA was isolated from mouse Achilles tendons and their entheses. Freshly dissected tissues were cut into small pieces, snap-frozen in liquid nitrogen, pulverized with a Mikro-Dismembrator U (Sartorius AG, Goettingen, Germany), and lysed in TRIzol Reagent (Life Technologies, Carlsbad, CA, USA). Total RNA in lysed tissues was isolated via phase separation after addition of chloroform/isoamyl alcohol 24:1 (Sigma-Aldrich) using a Phase Lock Gel (5 Prime GmbH, Hamburg, Germany). RNA in the upper aqueous phase was collected and purified with RNeasy MinElute Spin Columns (Qiagen Sciences, Germantown, MD, USA). Isolated total RNA (500 ng) was reverse-transcribed into cDNA using a SuperScript IV VILO Master Mix (Life Technologies). The relative abundances of genes of interest were determined by SYBR green real-time PCR using Qiagen (Table 1) or custom primers (Table 2). *Ipo8* was used as an endogenous reference gene. Changes in tendon gene expression were determined by the comparative Ct method and reported as relative mRNA abundance ($2^{-\Delta Ct}$) unless described elsewhere.

Statistical analysis

Two-way ANOVAs followed by Sidak's multiple comparisons or Fisher's LSD tests were used to compare the effects of age and strain on postnatal tendon and enthesis formation or the effects of activity and strain on tendon and enthesis mechanoresponsiveness. Two-tailed Student's *t* tests were used to compare the overall physical, metabolic, musculoskeletal, and tendon biomechanical properties between WT and cKO mice. The significance level was set at $p < 0.05$. All data are shown as box plots that include median and range (minimum, 25th percentile, 75th percentile, and maximum) unless otherwise specified.

Immunostaining and histomorphometry

Freshly dissected SS tendons attached to the humeral head and Achilles tendons attached to the calcaneus were fixed in 4% PBS and decalcified in 14% acid-free EDTA. The decalcified SS tendons were embedded in paraffin, sectioned in the coronal plane (5 μm thick), and stained with toluidine blue or Cx43 antibodies (Sigma-Aldrich, 1:2000 dilution) as previously described.[17] Decalcified Achilles tendons were embedded in Tissue-Tek OCT Compound, sectioned in the sagittal plane (8 μm thick), and stained with antibodies specific for Cx43, BrdU, or Gli1. Cx43 immunofluorescence staining was performed as described elsewhere.[17] BrdU immunohistochemistry was performed using a BrdU staining kit (Invitrogen, catalog number 933943) according to manufacturer's instructions. Sections were counterstained with hematoxylin. $BrdU^+$ cells at the enthesis region of Achilles tendon sections were counted blindly and expressed as a percentage of hematoxylin-stained cells within the region of interest. For Gli1 immunofluorescence staining, Achilles tendon sections were permeabilized in 0.2% Triton X-100 in PBS for 10 minutes and blocked in a blocking buffer containing 5% normal donkey serum and 0.05% Triton X-100 in PBS for 30 minutes. The sections were then incubated with rabbit anti-gli1 antibodies (OriGene, Rockville, MD, USA; 1:200 dilution) at 4°C overnight. After thorough washing, the sections were further incubated with Cy3-labeled donkey anti-rabbit antibodies (Jackson ImmunoResearch, West Grove, PA, USA; 1:400 dilution) for 1 hour and then mounted in Vectashield Antifade Mounting Medium with DAPI (Vector Laboratories, Inc., Burlingame, CA, USA). $Gli1^+$ cells at the enthesis region of Achilles tendon sections were counted blindly and expressed as a percentage of $DAPI^+$ cells within the region of interest.

Results

Expression and selective deletion of *Gja1* in the tendon and enthesis

Immunohistochemistry staining with anti-Cx43 antibodies demonstrated that, in addition to bone cells (red arrowheads in Fig. 1A), Cx43 was also strongly expressed by mouse tenocytes (black arrows in Fig. 1A) and entheseal fibrocartilage cells (black arrowheads in Fig. 1A). The Cre recombinase driven by the scleraxis promoter (ScxCre) was used to selectively delete the Cx43 gene *Gja1* from the tendon and enthesis.[24] The selectivity of this approach was validated by crossing the Ai14 Cre reporter mice[23] with *ScxCre*;*ScxGFP* mice that expressed the ScxGFP tendon reporter.[24] Results showed that ScxCre (red in Fig. 1B, B′) was expressed by the $ScxGFP^+$ tenocytes (arrows in Fig. 1B′) and entheseal cells (arrowheads in Fig. 1B′) but not the adjacent bone cells (Fig. 1B). The efficiency of *Gja1* deletion in the resulting cKO mice (*ScxCre*;$Gja1^{flox/-}$) was examined by Cx43

immunostaining on the Achilles tendon sections from these mice. The staining detected strong Cx43-positive signals in WT tendons (white arrows and open arrowheads in Fig. 1C) but not in cKO tendons (Fig. 1D). In WT tendons, Cx43 signals were found at the ends of elongated tenocytes (arrows in Fig. 1C; arrowheads indicate cell body) where two neighboring cells were likely in contact. Diffuse Cx43 signal was also detected in cells in the absence of obvious cell–cell contact (open arrows in Fig. 1C). The relative abundance of *Gja1* mRNA in the Achilles tendon and enthesis was further compared between WT and cKO mice by real-time PCR. Although the assay revealed robust *Gja1* expression in WT mice (ΔCt: 8.42 ± 0.72, $n = 8$), *Gja1* mRNA was only detected in two of eight cKO samples assessed (ΔCt: 13.58 and 17.37), thus confirming *Gja1* was effectively removed from tendon and enthesis cells in the cKO mouse model.

Gja1 deficiency in the tendon and enthesis impairs postnatal tendon enthesis formation and function

Gja1 tendon and enthesis deficiency only had a small effect on SS tendon CSA (Fig. 2A; $p = 0.037$ for strain by two-way ANOVA, $p = 0.79$ and 0.076 between WT and cKO at 4 and 8 weeks, respectively, by Sidak's multiple comparisons tests). However, *Gja1* deficiency significantly impaired postnatal SS tendon enthesis formation and function. Specifically, the volumes of mineralized fibrocartilage in cKO entheses were 30% and 20% smaller than those of WT entheses at the age of 4 and 10 weeks, respectively (Fig. 2B; $p = 0.001$ and $p < 0.001$ for the factor strain and age, respectively, by 2-way ANOVA; $p = 0.17$ and 0.003 between WT and cKO at 4 and 8 weeks, respectively, by Sidak's tests). Toluidine blue staining of 8-week SS tendon entheses revealed that WT entheseal cells were organized in columns in a direction largely parallel to the direction of muscle force (yellow boxes in Fig. 2C); this organization was disrupted in cKO entheses (open arrowheads in Fig. 2D). Moreover, the mechanical properties of cKO SS tendons were inferior to those of WT, showing a significant 20% reduction in maximum force (Fig. 2E; $p = 0.027$), a significant 30% reduction in stiffness (Fig. 2G; $p = 0.019$), and a trending 25% reduction of Young's modulus (Fig. 2H; $p = 0.099$) compared with WT tendons. Importantly, all tendons failed at the enthesis during biomechanical testing, supporting the conclusion that entheseal changes caused by *Gja1* deletion contributed to the inferior biomechanical properties. Additional functional evaluation was conducted in 10-week-old mice subjected to an intermediate-level treadmill running protocol. Compared with WT mice, cKO mice experienced difficulty in completing the running protocol, showing a 20-fold higher fail rate relative to their WT littermates (Fig. 2I; $p = 0.045$).

Gja1 deficiency in tendons and enthesis does not alter mouse size, strength, and physical activity

Enthesis development and mineralization are driven in large part by muscle loading.[4,5] To gain insights into the mechanisms of tendon and enthesis defects in cKO mice, we first compared body weight, maximum CSA of the SS muscle, and upper limb grip strength between WT and cKO mice. Although both WT and cKO mice showed expected increases in these parameters during postnatal development (Fig. 3A–C; $p < 0.001$ for the factor age by 2-way ANOVA), no significant differences were detected between the two mouse strains in body weight (Fig. 3A; $p = 0.26$), maximum SS muscle CSA (Fig. 3B; $p = 0.30$), and grip

strength (Fig. 3C; $p = 0.44$). Additionally, Cx43 defects have been associated with various cardiovascular conditions and scleraxis has also been reported in heart valve development,[25,26] which could limit mouse physical activity and thereby alter the mechanical loads on the developing enthesis. The activity levels of WT and cKO mice were therefore examined using metabolic cages. Results showed no apparent differences between the two strains in voluntary activity (Fig. 3D; $p = 0.16$), respiratory exchange ratio (RER; Fig. 3E; $p = 0.96$), and energy expenditure (Fig. 3F; $p = 0.12$). Collectively, the results support the conclusion that WT and cKO tendon entheses experienced similar loading environments during development.

The impact of *Gja1* deficiency in the tendon and enthesis on adjacent trabecular bone formation

The mechanical properties of the tendon enthesis are dictated in part by the bone underlying the fibrocartilaginous attachment. As shown in Fig. 1A, the subchondral/lamellar bone underneath the supraspinatus tendon enthesis is very thin, in contrast to the trabecular bone that extends from the enthesis to the growth plate. To determine if the impaired strength of tendon enthesis after *Gja1* deletion might be associated with alterations in adjacent bone formation, the trabecular bone microstructure and cortical properties at the humeral head were compared between WT and cKO mice. We observed significant 10% and 7% reductions in TV in 4-week- and 8-week-old cKO mice, respectively (Fig. 4A; $p = 0.006$ for mouse strain and $p < 0.0001$ for age, by 2-way ANOVA). No other bone parameters were significantly changed in cKO mice compared with WT mice (Figs. 4B–G, $p = 0.25$, 0.99, 0.55, 0.59, 0.36, and 0.062 for BV, BV/TV, TMD, Tb. N, Tb.Th, and Tb.Sp, respectively, by 2-way ANOVA). Although we did not directly examine the expression level of Cx43 in bone tissue in this study, Figs. 4A and 3A–C showed that the cKO mouse model did not exhibit the phenotype caused by Cx43 deficiency in the bone—an increase in total bone volume and reductions in body weight, skeletal muscle size, and grip strength.[17] The overall reduction in humeral bone size in the *Gja1* cKO mice is consistent with the reduction in size of the mineralized fibrocartilage of the SS enthesis, suggesting an association between Cx43 deficiency in tenocytes and fibrocartilage cells and adjacent bone formation.

Gja1 deficiency in the tendon and enthesis reduces entheseal anabolic responses to treadmill exercise

Given the importance of mechanical loading for enthesis formation and the role of Cx43 in regulating bone mechanoresponsiveness[9,12,13,16] and intracellular signaling,[14,15] we asked if Cx43 was necessary for tendon enthesis responses to mechanical stimulus. To address the question, mouse Achilles tendon entheses were loaded via treadmill running and their responses were compared between WT and cKO mice at the mRNA level (Fig. 5A–G). Moderate treadmill running led to a trending increase in expression of the tenogenic growth factor *Tgfb2*[27,28] (Fig. 5B; 1.5-fold, $p = 0.050$) in the WT Achilles tendons and entheses. Moreover, *Sox9*, a transcriptional factor necessary for enthesis formation,[29,30] was significantly increased by 2.2-fold in WT Achilles tendons and entheses after treadmill running (Fig. 5G; WT cage versus WT treadmill, $p = 0.039$). In contrast, no apparent changes were detected in the expression levels of any of the genes assessed in the Achilles tendons and entheses of cKO mice after treadmill running (Fig. 5A–G; cKO cage versus

cKO treadmill, $p = 0.99$, 0.42, 0.36, 0.72, 0.40, 0.19, and 0.18 for *A–G*, respectively). Comparing WT and cKO mice, the expression levels of *Tgfb2* and the tenogenic marker *Tnmd* in WT treadmill mice were 1.6- and 2.0-fold of those in cKO treadmill mice (Fig. 5B, F; $p = 0.050$ for *Tgfb2* and 0.053 for *Tnmd*). With regard to cage control mice, cKO mice expressed a higher-than-normal level of *Scx* (Fig. 5D; $p = 0.043$ for the factor strain by 2-way ANOVA and $p = 0.055$, cKO cage versus WT cage by Sidak's test), which was coupled with an increase in *Sox9* expression (Fig. 5G; cKO cage versus WT cage, 2.1-fold, $p = 0.062$). Together, there was a significant interaction between mouse strain and activity in regulating *Sox9* expression level in Achilles tendons and tendon entheses (Fig. 5G; $p = 0.019$ by two-way ANOVA). Similar interaction trends were also found in regulating *Tgfb2* (Fig. 2B; $p = 0.058$) and *Tnmd* (Fig. 5F; $p = 0.060$) expression in Achilles tendons and entheses.

At the tissue level, the anabolic response of entheseal cells to treadmill running were compared between WT and cKO mice at the Achilles tendon enthesis via an in vivo BrdU incorporation assay. BrdU-positive signals were subsequently detected by immunohistochemistry staining (Fig. 5H–L). The specificity of the staining was validated by confirming positive signals on a mouse small intestine section (Supplemental Fig. S1A) and by showing negative signals on an Achilles tendon enthesis section from a WT mouse that did not take BrdU (Supplemental Fig. S1B). In line with the gene expression results, the percentage of $BrdU^+$ proliferative cells (dark brown, indicated by black arrows in Fig. 5I–L) in the Achilles tendon entheses of WT cage mice was only 46% of that of the cKO cage mice (Fig. 5H, I, K; WT cage versus cKO cage, $p < 0.001$). Although treadmill running led to a twofold increase in the percentage of $BrdU^+$ entheseal cells in WT Achilles tendons (Fig. 5H–J; WT cage versus WT exercise, $p = 0.003$), the percentage of $BrdU^+$ entheseal cells was reduced by nearly 60% in the cKO mice subjected to the treadmill exercise (Fig. 5H, K, L; cKO cage versus cKO exercise, $p < 0.001$). As a result, the percentage of $BrdU^+$ entheseal cells in WT Achilles loaded via treadmill exercise was 2.2-fold of that in cKO Achilles tendons loaded via treadmill exercise (Fig. 5H, J, L; WT exercise versus cKO exercise, $p = 0.003$). Statistical analysis demonstrated a significant interaction between mouse strain and activity ($p < 0.001$ by 2-way ANOVA). Collectively, the results confirmed that *Gja1* deficiency in the tendon and enthesis reduced the anabolic response of entheseal cells to mechanical loading.

Gja1 deficiency in the tendon and enthesis affects treadmill exercise-induced Ihh/Gli1 signaling in the Achilles tendon and enthesis

With regard to the underlying mechanisms contributing to the malformation and deregulated mechanoresponsiveness of the *Gja1*-deficient enthesis, we considered the hedgehog/Gli1 signaling pathway, which has been linked to enthesis formation, biomechanical properties, and response to loading.[6–8] The expression levels of *Ihh*, the Ihh receptors *Ptch1* and *Smo*, and the downstream transcriptional factor *Gli1* in the Achilles tendon enthesis were compared between WT and cKO mice with and without treadmill exercise. Results showed that the level of *Ihh* expression in WT mice was increased by more than twofold after treadmill running (Fig. 6A; $p = 0.047$, WT cage versus WT exercise); in contrast, cKO mice expressed a higher-than-normal level of *Ihh* with cage activity (Fig. 6A; cKO cage versus

WT cage, 3.2-fold, $p = 0.003$), which was reduced by nearly 60% after treadmill exercise (Fig. 6A; cKO cage versus cKO exercise, $p = 0.011$). There was a significant interaction between mouse strain and activity regarding *Ihh* expression in the Achilles tendon enthesis ($p = 0.002$). No significant differences in *Ptch1*, *Smo*, and *Gli1* expressions were detected between the WT and the cKO mice, regardless of their activity level (Fig. 6B–D; $p = 0.55$, 0.52, and 0.80 for the factor strain, $p = 0.073$, 0.619, and 0.18 for the factor activity, and $p = 0.17$, 0.958, and 0.44 for the interaction between strain and activity, respectively).

At the tissue level, Gli1 immunostaining on sagittal sections of Achilles tendon entheses revealed that most of the $Gli1^+$ signal was co-localized with DAPI staining in the nuclei of enthesis cells (yellow arrows in Fig. 6E). Similar to the pattern of *Ihh* expression, $Gli1^+$ cells were rare in the entheses of WT mice with regular cage activity and treadmill running induced a nearly fourfold increase of $Gli1^+$ cells at the region (Fig. 6E, F; WT cage versus WT treadmill, $p = 0.002$); in contrast, cKO cage control mice showed a higher-than-normal percentage of $Gli1^+$ cells in their Achilles tendon entheses (Fig. 6E, F; WT cage versus cKO cage, $p = 0.003$), and no apparent change in the percentage of $Gli1^+$ cells was detected in Achilles tendon entheses of cKO mice after treadmill exercise (Fig. 6E, F; cKO cage versus cKO exercise, $p = 0.62$). Statistical analysis confirmed a significant interaction between mouse strain and activity with regard to Gli1 expression in Achilles tendon enthesis ($p = 0.009$ by 2-way ANOVA).

Discussion

Previous studies have reported the pattern of Cx43 expression in tendon.[19,20,31] Despite these reports, the in vivo function of Cx43, particularly in the enthesis, was largely unknown. Using a tendon and enthesis-specific mouse genetic model, this study investigated the roles of Cx43 in postnatal tendon enthesis formation and response to loading. Results revealed that Cx43 is necessary for the formation of a functional tendon enthesis and that it plays a key role in tendon enthesis mechanoresponsiveness. Specifically, *Gja1* deficiency in the tendon and enthesis compromised entheseal cell organization and mineralized fibrocartilage formation, leading to inferior tendon enthesis strength. Furthermore, mice lacking Cx43 in the tendon and enthesis showed reduced mechanoresponsiveness and limited ability to perform treadmill running. These effects were likely caused by this deletion and not due to altered off-target loading effects, as no apparent differences were found between WT and cKO mice in body weight, cage activity, key metabolic indexes, muscle CSA, grip strength, and major trabecular bone properties.

Using treadmill running to modify in vivo loading at the tendon enthesis, we found a dual role of Cx43 in regulating enthesis anabolic responses to mechanical loading. Results showed that loading via treadmill exercise prompted an anabolic response in the tendon entheses of WT mice, and this response was attenuated after ablation of Cx43 in the enthesis. These findings support the conclusion that Cx43 in the tendon and enthesis is involved in the tissue's response to mechanical loads. In line with this idea, an in vivo study reported that absence of Cx43 in bone cells resulted in activation of periosteal bone formation at lower strains than in wild-type bones,[32] whereas others showed that gap junction function is required for flexor tendon anabolic responses to mechanical loading in

an ex vivo model.[21] With the increases in muscle size and activity during postnatal development, the enthesis experiences a rapid increase in mechanical load during growth and maturity, and this loading is necessary for the formation of a functional attachment.[4,5] Therefore, the structural and functional defects observed in postnatal enthesis after *Gja1* deletion are likely the result of deregulated enthesis responses to mechanical loading.

Results also support the hypothesis that entheseal mechanoresponsiveness is coupled to activation of the hedgehog/Gli1 signaling pathway and that Cx43 is required for this response. These findings are in line with the previously described role of hedgehog/Gli1 signaling in regulating enthesis formation[6–8] and the correlation between the presence and absence of Cx43 and entheseal anabolic responses described in the current study. In our prior work, we showed the pattern of mineralization at the neonatal tendon enthesis[33] and the necessity of Gli1+ cells in driving fibrocartilage mineralization.[8] Consistently, in this study Gli1-positive signals were frequently detected in the entheseal cells near the tidemark in WT mice, whereas this pattern was not evident in cKO mice. Interestingly, our results showed that $Gli1^+$ cells in the WT enthesis increased after treadmill exercise, whereas the expression level of *Gli1* gene in the Achilles tendon-enthesis unit was not altered. This discrepancy likely resulted from a difference in tissue/cell specificity between the two assays. The tissue samples for gene expression analysis contain both tendon and enthesis tissues, including paratenon, whereas the Gli1 immunostaining and histomorphometry was enthesis cell-specific. The presence of RNA from tenocytes and paratenon cells could affect qPCR experimental outcomes and conclusions. Alternatively, Gli1 expression may be regulated post-transcriptionally. Future cell type–specific gene expression studies would be helpful to address this inconsistency.

Cx43 was selectively removed from both the tendon and its enthesis using ScxCre. Unlike the enthesis, the overall structure of the tendon was not affected by *Gja1* deletion. Tendon CSA and tenocyte organization were similar when comparing WT and cKO mice, implying that Cx43 is not required for defining tendon microarchitecture. Therefore, the reduced mechanical properties in the cKO mice were likely due to alterations at the enthesis, not the tendon midsubstance; this is consistent with the observation that all samples failed via avulsion of mineralized tissue at the tendon-bone interface during biomechanical testing.

In one set of experiments, young adult mice were subjected to a treadmill running protocol to evaluate the impact of Cx43 on enthesis mechanoresponsiveness. These experiments revealed that young cKO mice could not consistently complete the protocol. Therefore, in a second set of experiments, older mice were subjected to a more modest running protocol to evaluate enthesis mechanoresponsiveness in the absence of Cx43. Furthermore, a relatively short-duration treadmill running protocol was chosen, as Cx43 was expected to play a role in rapidly transducing mechanical stimuli into biochemical signals. Consistent with this reasoning, gene expression analysis focused on genes known to be involved in early mechanotransduction events during tendon and enthesis formation. This approach successfully identified that Sox9 and hedgehog/Gli1 are sensitive to Cx43 deletion. A follow-up in vivo study is necessary to define the interaction between Cx43 and hedgehog/Gli1 signaling for enthesis mechanoresponsiveness. Furthermore, an exploratory

transcriptomics analysis is necessary to define other regulatory elements that connect Cx43 with enthesis development and mechanotransduction.

In summary, this in vivo study revealed that Cx43 in the tendon and enthesis is necessary for proper formation of a functional tendon-to-bone attachment. Results further demonstrate a contributory role of Cx43 in regulating enthesis mechanoresponses under treadmill loading conditions. Knowledge gained from this study may be used for future development of mechanoregulation-based therapies for enthesis-related disorders.

Supplementary Material

Refer to Web version on PubMed Central for supplementary material.

Acknowledgments

This study is supported by NIH R01 AR055580 and NIH P30 AR057235.

References

1. Lu HH, Thomopoulos S. Functional attachment of soft tissues to bone: development, healing, and tissue engineering. Annu Rev Biomed Eng. 2013;15:201–26. [PubMed: 23642244]
2. Genin GM, Thomopoulos S. The tendon-to-bone attachment: unification through disarray. Nat Mater. 2017;16:607–8. [PubMed: 28541313]
3. Zelzer E, Blitz E, Killian ML, Thomopoulos S. Tendon-to-bone attachment: from development to maturity. Birth Defects Res C Embryo Today. 2014;102:101–12. [PubMed: 24677726]
4. Thomopoulos S, Kim HM, Rothermich SY, Biederstadt C, Das R,Galatz LM. Decreased muscle loading delays maturation of the tendon enthesis during postnatal development. J Orthop Res. 2007;25: 1154–63. [PubMed: 17506506]
5. Schwartz AG, Lipner JH, Pasteris JD, Genin GM, Thomopoulos S. Muscle loading is necessary for the formation of a functional tendon enthesis. Bone. 2013;55:44–51. [PubMed: 23542869]
6. Dyment NA, Breidenbach AP, Schwartz AG, et al. Gdf5 progenitors give rise to fibrocartilage cells that mineralize via hedgehog signaling to form the zonal enthesis. Dev Biol. 2015;405:96–107. [PubMed: 26141957]
7. Breidenbach AP, Aschbacher-Smith L, Lu Y, et al. Ablating hedgehog signaling in tenocytes during development impairs biomechanics and matrix organization of the adult murine patellar tendon enthesis. J Orthop Res. 2015;33:1142–51. [PubMed: 25807894]
8. Schwartz AG, Long F, Thomopoulos S. Enthesis fibrocartilage cells originate from a population of hedgehog-responsive cells modulated by the loading environment. Development. 2015;142:196–206. [PubMed: 25516975]
9. Plotkin LI, Speacht TL, Donahue HJ. Cx43 and mechanotransduction in bone. Curr Osteoporos Rep. 2015;13:67–72. [PubMed: 25616771]
10. Civitelli R Cell-cell communication in the osteoblast/osteocyte lineage. Arch Biochem Biophys. 2008;473:188–92. [PubMed: 18424255]
11. Stains JP, Civitelli R. Cell-to-cell interactions in bone. Biochem Biophys Res Commun. 2005;328:721–7. [PubMed: 15694406]
12. Jiang JX, Cherian PP. Hemichannels formed by connexin 43 play an important role in the release of prostaglandin E(2) by osteocytes in response to mechanical strain. Cell Commun Adhes. 2003;10:259–64. [PubMed: 14681026]
13. Genetos DC, Kephart CJ, Zhang Y, Yellowley CE, Donahue HJ. Oscillating fluid flow activation of gap junction hemichannels induces ATP release from MLO-Y4 osteocytes. J Cell Physiol. 2007;212:207–14. [PubMed: 17301958]

14. Leithe E, Mesnil M, Aasen T. The connexin 43 C-terminus: a tail of many tales. Biochim Biophys Acta Biomembr. 1860;2018:48–64.
15. Moorer MC, Hebert C, Tomlinson RE, Iyer SR, Chason M, Stains JP. Defective signaling, osteoblastogenesis and bone remodeling in a mouse model of connexin 43 C-terminal truncation. J Cell Sci. 2017;130:531–40. [PubMed: 28049723]
16. Grimston SK, Watkins MP, Stains JP, Civitelli R. Connexin43 modulates post-natal cortical bone modeling and mechano-responsiveness. Bonekey Rep. 2013;2:446. [PubMed: 24422141]
17. Shen H, Grimston S, Civitelli R, Thomopoulos S. Deletion of connexin43 in osteoblasts/osteocytes leads to impaired muscle formation in mice. J Bone Miner Res. 2015;30:596–605. [PubMed: 25348938]
18. Xu H, Gu S, Riquelme MA, et al. Connexin 43 channels are essential for normal bone structure and osteocyte viability. J Bone Miner Res. 2015;30:436–48. [PubMed: 25270829]
19. McNeilly CM, Banes AJ, Benjamin M, Ralphs JR. Tendon cells in vivo form a three dimensional network of cell processes linked by gap junctions. J Anat. 1996;189:593–600. [PubMed: 8982835]
20. Schwab W, Hofer A, Kasper M. Immunohistochemical distribution of connexin 43 in the cartilage of rats and mice. Histochem J. 1998;30:413–9. [PubMed: 10192540]
21. Banes AJ, Weinhold P, Yang X, et al. Gap junctions regulate responses of tendon cells ex vivo to mechanical loading. Clin Orthop Relat Res. 1999;367(Suppl):S356–70.
22. Maeda E, Kimura S, Yamada M, Tashiro M, Ohashi T. Enhanced gap junction intercellular communication inhibits catabolic and pro-inflammatory responses in tenocytes against heat stress. J Cell Commun Signal. 2017;11:369–80. [PubMed: 28601938]
23. Madisen L, Zwingman TA, Sunkin SM, et al. A robust and high throughput Cre reporting and characterization system for the whole mouse brain. Nat Neurosci. 2010;13:133–40. [PubMed: 20023653]
24. Pryce BA, Brent AE, Murchison ND, Tabin CJ, Schweitzer R. Generation of transgenic tendon reporters, ScxGFP and ScxAP, using regulatory elements of the scleraxis gene. Dev Dyn. 2007;236:1677–82. [PubMed: 17497702]
25. Michela P, Velia V, Aldo P, Ada P. Role of connexin 43 in cardiovascular diseases. Eur J Pharmacol. 2015;768:71–6. [PubMed: 26499977]
26. Levay AK, Peacock JD, Lu Y, et al. Scleraxis is required for cell lineage differentiation and extracellular matrix remodeling during murine heart valve formation in vivo. Circ Res. 2008;103:948–56. [PubMed: 18802027]
27. Pryce BA, Watson SS, Murchison ND, Staverosky JA, Dünker N, Schweitzer R. Recruitment and maintenance of tendon progenitors by TGFbeta signaling are essential for tendon formation. Development. 2009;136:1351–61. [PubMed: 19304887]
28. Havis E, Bonnin MA, Esteves de Lima J, Charvet B, Milet C, Duprez D. TGFβ and FGF promote tendon progenitor fate and act downstream of muscle contraction to regulate tendon differentiation during chick limb development. Development. 2016;143:3839–51. [PubMed: 27624906]
29. Sugimoto Y, Takimoto A, Akiyama H, et al. Scx+/Sox9+ progenitors contribute to the establishment of the junction between cartilage and tendon/ligament. Development. 2013;140:2280–8. [PubMed: 23615282]
30. Blitz E, Sharir A, Akiyama H, Zelzer E. Tendon-bone attachment unit is formed modularly by a distinct pool of Scx- and Sox9-positive progenitors. Development. 2013;140:2680–90. [PubMed: 23720048]
31. Coleman CM, Loredo GA, Lo CW, Tuan RS. Correlation of GDF5 and connexin 43 mRNA expression during embryonic development. Anat Rec A Discov Mol Cell Evol Biol. 2003;275:1117–21. [PubMed: 14613311]
32. Grimston SK, Watkins MP, Brodt MD, Silva MJ, Civitelli R. Enhanced periosteal and endocortical responses to axial tibial compression loading in conditional connexin43 deficient mice. PLoS One. 2012; 7:e44222. [PubMed: 22970183]
33. Schwartz AG, Pasteris JD, Genin GM, Daulton TL, Thomopoulos S. Mineral distributions at the developing tendon enthesis. PLoS One. 2012;7:e48630. [PubMed: 23152788]

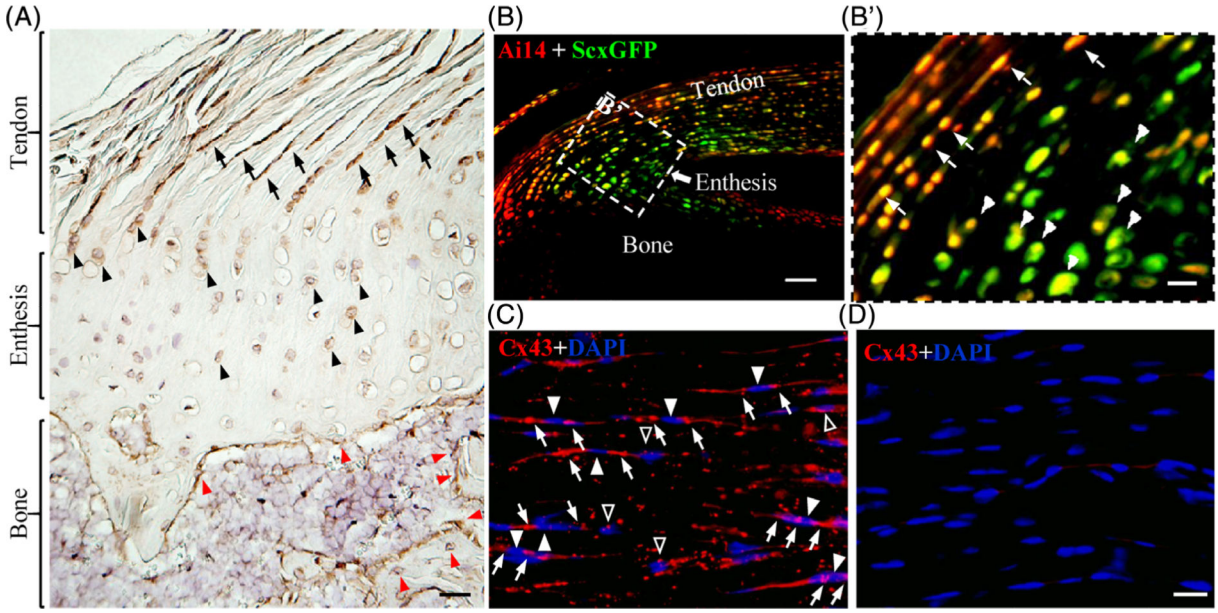

Fig. 1.

Expression and selective deletion of Cx43 in tendon and enthesis cells. (*A*) representative image of a coronal section of mouse supraspinatus tendon and enthesis (4 weeks) stained with antibodies against Cx43 (dark brown). Black arrows, black arrowheads, and red arrowheads denote tenocytes, entheseal fibrocartilage cells, and osteoblasts or osteocytes, respectively. Scale bar = 50 μm. (*B*, *B*′) Representative image of a sagittal section of mouse Achilles tendon and enthesis from a 2-week-old *Ai14*;*ScxCre*;*ScxGFP* reporter mouse. (*B*′) Enlarged view of the boxed region in *B*. White arrows and arrowheads in *B*′ indicate tenocytes and fibrocartilage cells, respectively. Scale bars = 100 μm and 20 μm in *B* and *B*′, respectively. (*C*, *D*) Representative images of Achilles tendon sections from 4-week-old WT (*C*) and KO (*D*) mice stained with anti-Cx43 antibodies (red) and DAPI (blue). White arrowheads in *C* indicate the cell bodies of tenocytes expressing Cx43. White arrows and open arrowheads in *C* denote Cx43-positive signals at the two ends and the sides of spindle-shaped tenocytes, respectively. Scale bar = 20 μm (*C*, *D*).

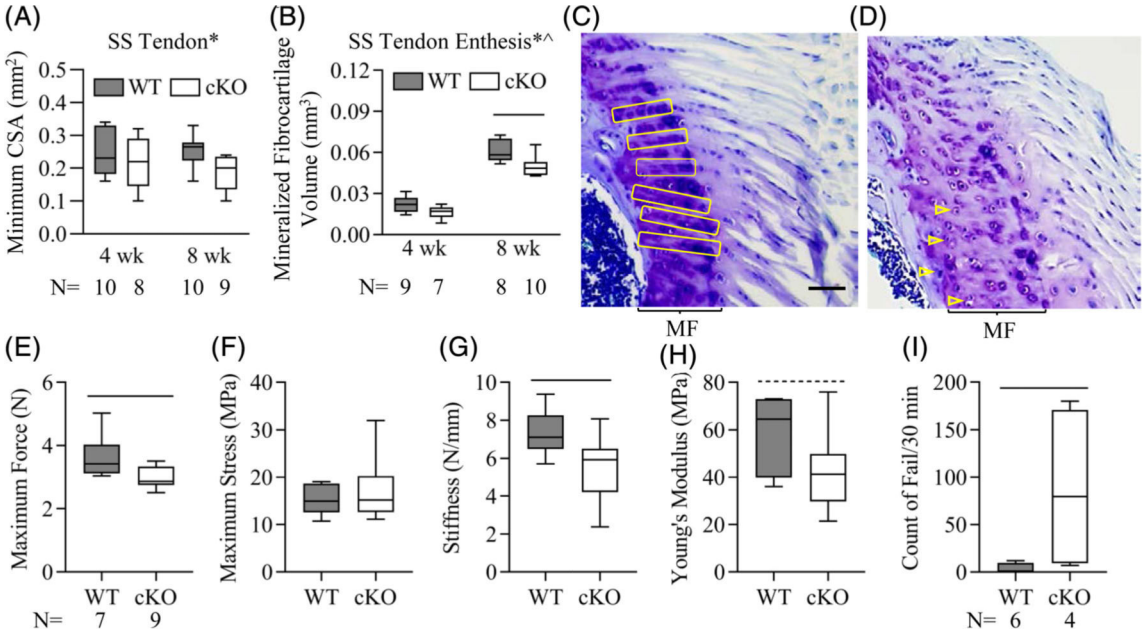

Fig. 2.

Gja1 tendon and enthesis deficiency impaired mouse tendon enthesis structure and strength and animal physical performance. (*A*, *B*) Impact of *Gja1* tendon and enthesis deficiency on mouse supraspinatus (SS) tendon (*A*) and enthesis (*B*) structure. ^and *, $p < 0.05$ for age and strain, respectively, by 2-way ANOVA; —, $p < 0.05$ between indicated groups by Sidak's multiple comparisons test. (*C*, *D*) Representative images of toluidine blue-stained sections of SS tendon and enthesis from 8-week-old WT (*C*) and cKO (*D*) mice. Scale bar = 50 μm (*C*, *D*). MF = mineralized fibrocartilage. Arrangement of entheseal cells indicated by yellow boxes and arrowheads. (*E–H*) Impact of *Gja1* tendon and enthesis deficiency on the biomechanical properties of SS tendons from 8-week-old WT and cKO mice. —, $p < 0.05$ and -----, $p < 0.1$ between the indicated groups by Student's *t* tests. The sample size (*N*) indicated in *E* applies to *E–H*. (*I*) Counts of falls of 10-week-old WT and cKO mice in a 30-minute session of modest treadmill running. —, $p < 0.05$ by Student's *t* test.

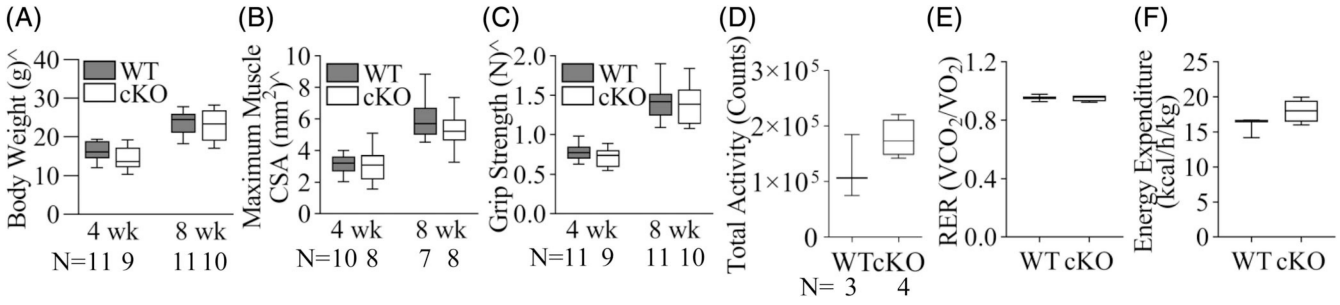

Fig. 3.

There were no apparent changes in mouse body weight (*A*), supraspinatus muscle maximum cross-sectional area (CSA; *B*), upper limb grip strength (*C*), total voluntary activities (*D*), respiratory exchange ratio (RER; *E*), and energy expenditure (*F*) in mice with *Gja1* tendon and enthesis deficiency. ^, 2-way ANOVA, $p < 0.05$ for age. The sample size (*N*) in *D* applies to *D*–*F*.

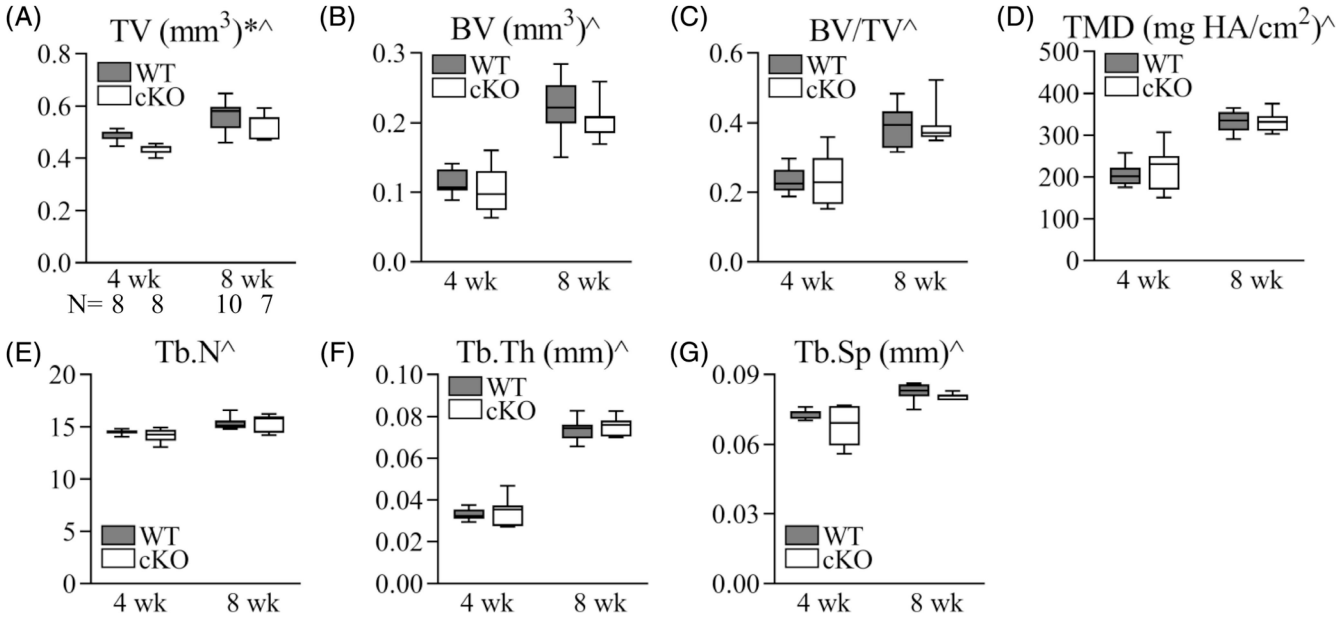

Fig. 4.

The impact of *Gja1* tendon and enthesis deficiency on the trabecular bone properties of the humeral head. (*A*) Total volume (TV); (*B*) bone volume (BV); (*C*) bone and total volume ratio (BV/TV); (*D*) tissue mineral density (TMD); (*E*) trabecular number (Tb.N); (*F*) trabecular thickness (Tb.Th); (*G*) trabecular space (Tb.Sp). * and ^, 2-way ANOVA, $p < 0.05$ for strain and age, respectively. The sample size (*N*) in *A* applies to *A*–*G*.

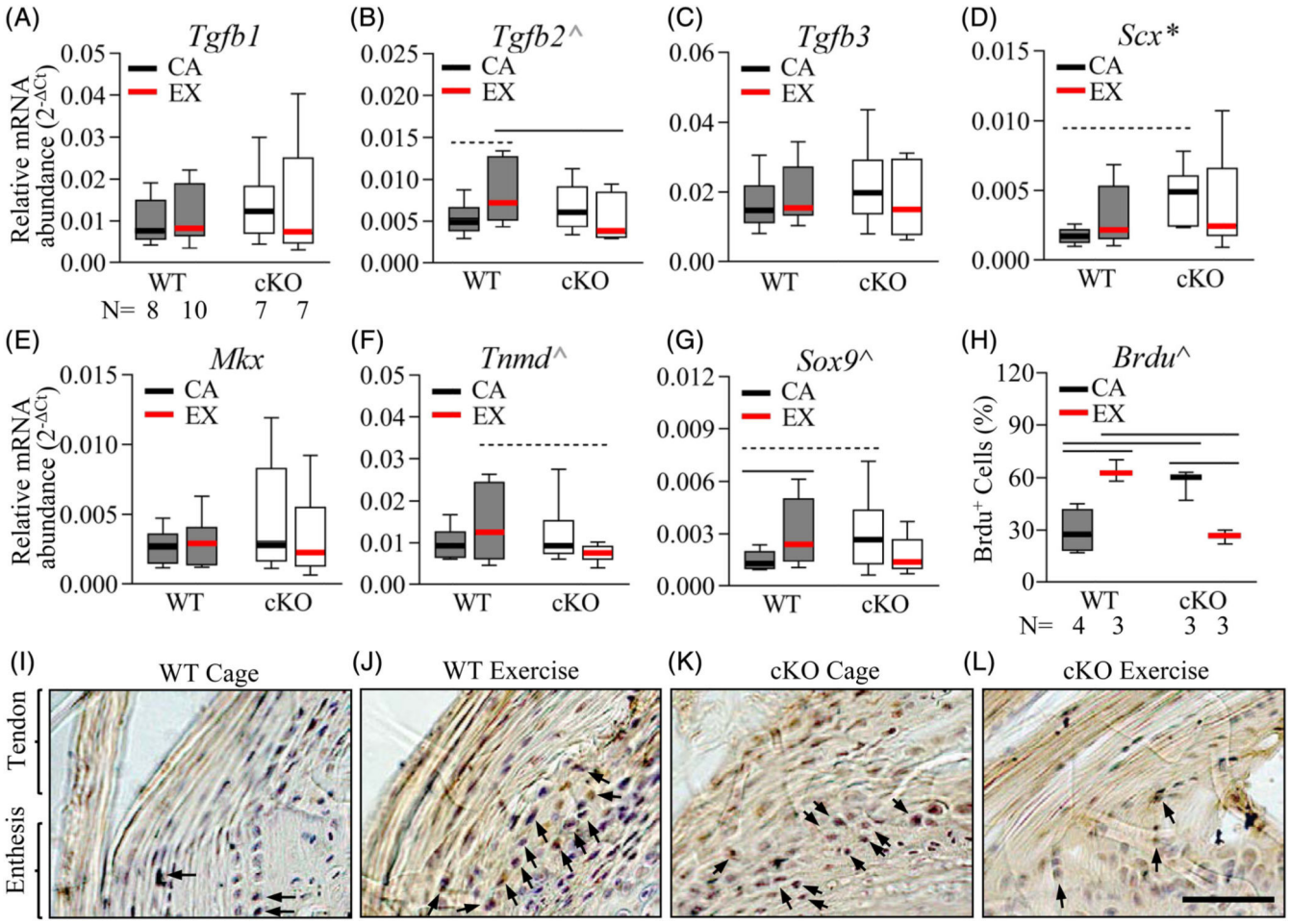

Fig. 5.

Gja1 deficiency in the tendon and enthesis impaired tissue responses to treadmill exercise. (*A-G*) Relative abundances of genes involved in tenogenesis and enthesis formation in the Achilles tendon and enthesis of WT and cKO mice with treadmill exercise (EX) or cage activity (CA). *, 2-way ANOVA, $p < 0.05$ for the factor strain; ^, 2-way ANOVA, $p < 0.05$ (black) and 0.1 (grey), for the interaction between activity and strain; — and -----, $p < 0.05$ and 0.1 by SNK post hoc tests between the indicated groups, respectively. The sample size (N) in *A* applies to *A-G*. (*H-L*) Histomorphometry (*H*) and the corresponding representative images (*I-L*) of $BrdU^+$ (in dark brown) entheseal cells in WT and cKO Achilles tendons with treadmill exercise (EX) or cage activity (CA). Black arrows indicate $BrdU^+$ entheseal cells. ^, 2-way ANOVA, $p < 0.05$ for the interaction between activity and strain. —, $p < 0.05$, between the indicated groups. Scale bar in *L*, 50 μm, applied to *I-L*.

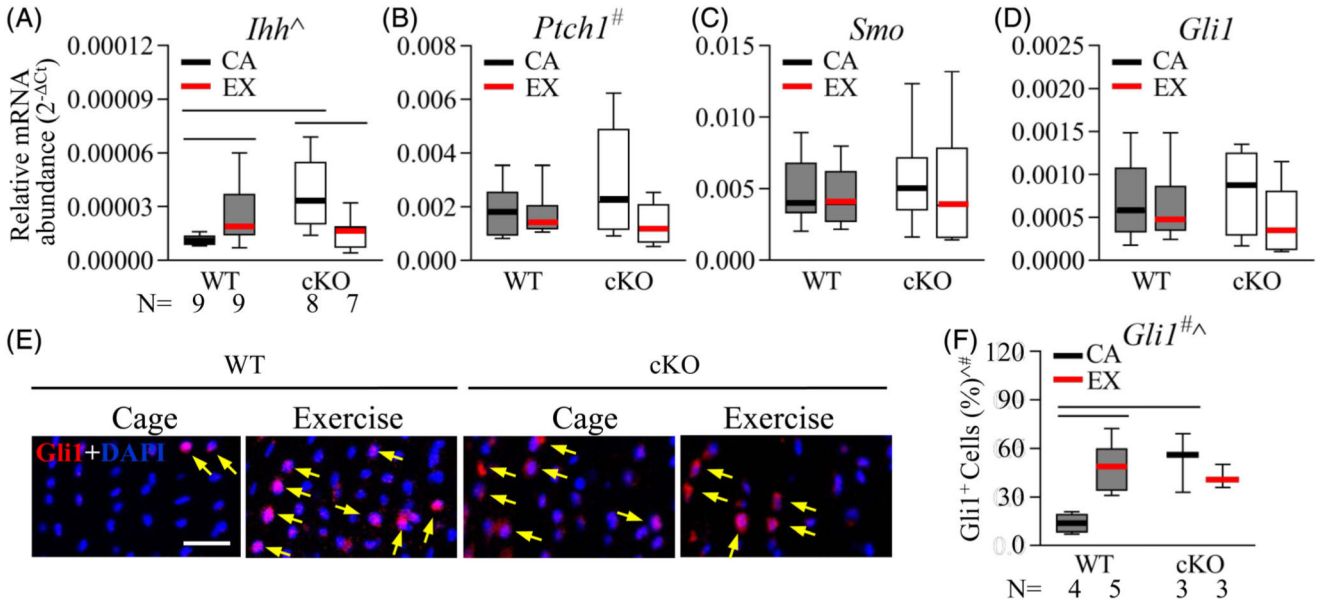

Fig. 6.

Gja1 deficiency in the tendon and enthesis altered treadmill exercise-induced hedgehog signaling at the Achilles tendon enthesis. (*A-D*), Relative abundances of genes involved in hedgehog signaling in the Achilles tendon and enthesis of WT and cKO mice with treadmill exercise (EX) or cage activity (CA). ^, $p < 0.05$ for the interaction between mouse activity and strain by 2-way ANOVA; #, $p < 0.1$ for the factor activity by 2-way ANOVA; —, $p < 0.05$ by Fisher's LSD tests between the indicated groups. (*E*, *F*) Representative fluorescence images (*E*) and quantification (*F*) of Gli1 (indicated with yellow arrows) and DAPI nuclear staining on Achilles tendon entheses from mice with treadmill exercise (EX) or cage activity (CA). Scale bar, 20 μm. # and ^, 2-way ANOVA, $p < 0.05$ for the factor activity and the interaction between activity and strain, respectively; —, $p < 0.05$ between indicated groups by Fisher's LSD tests.

Table 1.

Commercial Primers Used for Real-Time PCR

Gene symbol	Gene name	Assay number	Accession number	Amplicon (nt)
Gja1	gap junction protein, alpha 1	QT00173635	NM_010288	93
Gli1	GLI-Kruppel family member GLI1	QT00173537	NM_010296	74
Mkx	mohawk homeobox	QT00155610	NM_177595	106
Ptch1	patched 1	QT00149135	NM_008957	73
Scx	scleraxis	QT00166271	NM_198885	67
Smo	smoothened	QT00494683	NM_176996	104
Sox9	SRY (sex determining region Y)-box 9	QT00163765	NM_011448	124
Tgfb1	transforming growth factor, beta 1	QT00145250	NM_011577	145
Tgfb2	transforming growth factor, beta 2	QT00106806	NM_009367	109
Tgfb3	transforming growth factor, beta 3	QT00166838	NM_009368	86
Tnmd	tenomodulin	QT00126427	NM_022322	100

Table 2.

Custom Primers Used for Real-Time PCR

Gene symbol	Accession number	Forward primer	Reverse primer	Amplicon (nt)
Ihh	NM_010544	tgcattgctctgtcaagtctg	gctccccgttctctaggc	93
Ipo8	NM_001081113.1	cacattgtcgctcgtctctt	acctgttgaattcccactgc	112